Rock and Soil Mechanics

Volume 41 | Issue 11 Article 3

4-8-2021

An investigation of the mechanical properties of sandstone under coupled static and dynamic loading

Lei WEN
Mechanics Engineering Department, Shijiazhuang Tiedao University, Shijiazhang, Hebei 050043, China

Xu-li LIANG
School of Exploration Technology and Engineering, Hebei GEO University, Shijiazhuang, Hebei 050031, China

Wen-jie FENG
Mechanics Engineering Department, Shijiazhuang Tiedao University, Shijiazhang, Hebei 050043, China

Wei WANG
School of Civil Engineering, Shijiazhuang Tiedao University, Shijiazhang, Hebei 050043, China

See next page for additional authors

Custom Citation

WEN Lei, LIANG Xu-li, FENG Wen-jie, WANG Wei, WANG Liang, CHANG Jiang-fang, YUAN Wei, . An investigation of the mechanical properties of sandstone under coupled static and dynamic loading[J]. Rock and Soil Mechanics, 2020, 41(11): 3540-3552.

An investigation of the mechanical properties of sandstone under coupled static and dynamic loading

Authors

Lei WEN, Xu-li LIANG, Wen-jie FENG, Wei WANG, Liang WANG, Jiang-fang CHANG, and Wei YUAN

Rock and Soil Mechanics 2020 41(11): 3540−3552 ISSN 1000−7598
https: //doi.org/10.16285/j.rsm.2020.5214 rocksoilmech.researchcommons.org/journal

An investigation of the mechanical properties of sandstone under coupled static and dynamic loading

WEN Lei[1], LIANG Xu-li[3], FENG Wen-jie[1], WANG Wei[2], WANG Liang[2], CHANG Jiang-fang[1], YUAN Wei[2]

1. Mechanics Engineering Department, Shijiazhuang Tiedao University, Shijiazhang, Hebei 050043, China
2. School of Civil Engineering, Shijiazhuang Tiedao University, Shijiazhang, Hebei 050043, China
3. School of Exploration Technology and Engineering, Hebei GEO University, Shijiazhuang, Hebei 050031, China

Abstract: Through the application of SHPB (split Hopkinson pressure bar) test, this research firstly analyzed the law of damage under the cyclical impact on grey sandstone samples with the condition of static load. After that, to obtain the sample failure mode and speculate the relationship between dynamic stress and strain, the static-dynamic loading experiments on pre-damaged rock samples were also performed. Finally, based on the principle of strain equivalence, the total damage variable under the condition of static-dynamic loading was analyzed to derive the damage evolution equation to explain the relation of damage constitutive. Based on above tests, the research suggests: (1) the damage variable of rock sample can be divided into three stages during the process of cyclical impact, which are rapid increase, low-speed development and high-speed development, meanwhile, a higher axial pressure will lead to a lower damage variable in the stage of low-speed development; (2) compared with pre-damaged sample, the effect of strain rate enhancement on intact samples is more significant under the same condition; (3) the joint impact of pre-damaged variable (D_{01}) and static-load damage variable (D_{02}) might be negative, which therefore explained the fact that the dynamic strength increases with the static pressure under the condition of static-dynamic loading; (4) the constructed constitutive relation is also in perfect agreement with the curve of test value, which can in turn show a consistency between the macro- and micro- damage of the rock and then reflect the nonlinear influence of cyclical impact and static loading on total damage development.

Keywords: split Hopkinson pressure bar test; damage variable; cyclical impact; static-dynamic loading experiments; constitutive relation

1 Introduction

The surrounding rock of mines, tunnels, etc. is under static load, and may be affected by nearby blasting construction, mechanical vibration, and other dynamic loads. These dynamic loads are often applied multiple times or cyclically[1], which will cause gradual damage to the surrounding rock before macroscopic destruction is observed. This kind of pre-damaged rock will continue to bear the corresponding static load, and macroscopic failure will occur under a certain strong impact load. Therefore, studying the cyclic impact of rock under static load conditions and mechanical properties of this pre-damaged rock under the corresponding coupled dynamic and static loading has important theoretical significance and also useful in engineering applications.

When the rock is disturbed by external force, certain characteristics of internal mesostructure will vary with time, which is manifested as the generation and expansion of micro-cracks. These micro-cracks gradually develop with time[2]. At present, many scholars have studied the damage evolution law of rock under cyclic impact based on indicators such as acoustic emission, acoustic wave velocity, and elastic modulus. For example, Fan et al.[3] studied the relationship between sandstone wave velocity and the number of cyclic impacts. They found that the wave velocity decreases with the increase of the number of cyclic impacts, and this trend can be divided into three stages: initial rapid attenuation, stable attenuation, and accelerated attenuation. Lu[4] and Mei [5] found that rock damage is catastrophic under cyclic loading conditions. The degree of damage after the initial or first impact is the largest, and the damage degree of subsequent impact gradually decreases. The value of the damage variable rapidly becomes larger when the sample is critically damaged. LÜ et al.[6] used the Split Hopkinson Pressure Bar) (SHPB) to carry out cyclic impact tests on sandstone to study the influence of confining pressure on rock damage. Xiao et al.[7] proposed an inverted S-shaped damage cumulative evolution model based on the deformation characteristics of rock under cyclic static loading, and studied the effects of initial damage, stress amplitude, loading waveform and frequency on the fatigue mechanical properties of rock. It can be seen that researchers have studied the changes in the mechanical properties and the degree of damage of the rock by simple cyclic impact. A preliminary study has also been made on the degree of rock damage under the influence of confining pressure. However, there are only few studies on the damage characteristics of cyclic impact under pre-axial compression.

It is more reasonable to study the coupled dynamic and static strength and deformation properties of rocks

Received: 9 January 2020 Revised: 13 April 2020
This work was supported by the Natural Science Foundation of Hebei Province (E2018210066), the Postdoctoral Science Foundation of China (2018M631758) and the National Natural Science Foundation of China (51979170).
First author: WEN Lei, male, born in 1983, PhD, Assoiate Professor, mainly engaged in the teaching and research of rock mechanics. E-mail: WL0921@126.com
Corresponding author: FENG Wen-kai, male, born in 196, PhD, Professor, PhD supervisor, research interests: fracture mechanics. E-mail: wjfeng9999@126.com

under pre-static stress conditions than to study the effects of static or dynamic loads on rocks[8]. Regarding the coupled dynamic and static loads of SHPB, since Christenson et al. [9] conducted the first dynamic load test of rock under confining pressure in 1972, scholars at home and abroad have continuously improved the SHPB device and carried out several three-dimensional rock impact loading tests, and achieved a series of research results [10–16]. Liu et al.[13] used SHPB test equipment to conduct a one-dimensional coupled dynamic and static loading test study on coal and rock. Wen et al.[14] employed SHPB equipment with a diameter of 50 mm and capable of applying axial pressure, coupled with numerical simulation to study the dynamic mechanical properties of rocks under preloaded static loading after freezing and thawing. Yin[15] performed a dynamic and static coupling loading mechanical characteristic test of rock after temperature damage. Yang et al.[16] carried out a series of one-dimensional dynamic and static coupling loading tests on the mechanical properties, permeability, wave velocity and acoustic emission of the sample using the proposed coupled static-dynamic-static loading mode. At present, researchers have carried out a variety of coupled dynamic and static loading tests of rocks after freezing and thawing and high temperature damage, but there are very few rock coupled dynamic and static loading tests after cyclic impact damage, especially for the whole process of cyclic impact, pre-static load, and impact dynamic load damage.

In this study, a 50 mm diameter SHPB is used to carry out a cyclic impact test with pre-static axial compression on the rock to induce initial damage to the sample. The SHPB is again used to load the cyclic impact damage sample with a combination of dynamic and static loading to obtain the failure mode and dynamic stress–strain relationship of the sample and other indicators, to establish the damage evolution equation and damage constitutive relationship during the whole process. The findings in this paper can provide guidance for revealing the failure mechanism of dynamic and static loading of pre-damaged rock, and provide a theoretical basis for analyzing the stability of surrounding rock mass disturbed by dynamic load.

2 Test procedure and basic physical and mechanical properties of the sample

2.1 Test method

In this paper, medium-fine-grained grey sandstone is selected for the experiment. The sample is made into two types of cylinders with a diameter of 50 mm and a height of 100 or 50 mm, respectively. First, remove the specimens with macroscopic cracks, and then use the wave velocity meter to remove the samples with large difference in longitudinal wave velocity to complete the specimen screening. A total of 1 group is required for samples with a height of 100 mm. Samples with a height of 50 mm are divided into 12 groups, each of which is 3 to 4 pieces as a group. The finished samples are shown in Fig. 1.

Fig. 1 Samples of grey sandstone for tests

The test was carried out in the Engineering Mechanics Laboratory of Shijiazhuang Railway University. High-precision electronic balance, vernier caliper, electric heating blast drying oven and vacuum saturated water equipment were used to test basic physical indicators such as rock dry density and saturated water absorption. Hydraulic servo rigidity testing machine was used for uniaxial compression test. The SHPB, which can apply axial pressure, is used for the cyclic impact test and the coupled dynamic and static loading test. The incident rod, transmission rod, and absorption rod of the SHPB system are all 50 mm in diameter and 3 000, 2 000, and 1 000 mm in length. They are made of 40Cr alloy steel, with a density of 7 810 kg/m^3 and a longitudinal wave velocity of 5 410 m/ s, the elastic modulus is 210 GPa, and the SHPB test device is shown in Fig. 2. The rock acoustic wave meter (model: HS-YS4A) is used to test the longitudinal wave velocity of the sample before and after cyclic impact and the wave velocity during uniaxial loading. The HY-YS4A rock acoustic wave parameter tester consists of a micro-control host, high-voltage excitation, signal acquisition and multi-component piezoelectric transducers and other modules, with wide frequency bandwidth and high sensitivity. It can test the longitudinal wave velocity of rock samples and the wave velocity under uniaxial loading. The wave velocity test during uniaxial loading is shown in Fig. 3.

Fig. 2 SHPB test equipment

The dry, saturated, and uniaxial compression tests are carried out according to the relevant regulations [17], and the SHPB test is carried out according to the method recommended by the rock dynamics related test technology compiled by the Rock Dynamics Professional Committee of the International Society of Rock Mechanics and Rock Engineering[18]. The main test steps are as follows:

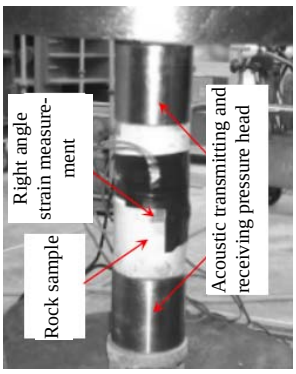

Fig. 3 Wave velocity test during loading

(1) Basic physical index test. The samples are screened, numbered, and grouped. The samples are forced to be saturated using the vacuum saturation device. The vacuum pressure is set to –0.1 MPa, and the time is set to 6 h. After that, samples are soaked for 24 h to measure the saturated mass of samples. Put the sample in an electric heating blast drying oven (temperature 105 ℃) for 48 h, weigh the sample again, and measure the size of the sample. Calculate the dry density and saturated water absorption of the sample.

(2) Test of sample wave velocity evolution after cyclic impact. Use SHPB equipment to cyclically strike 4 groups of 50 mm high specimens under different axial pressures (0, 15, 25, 35 MPa). After each impact, measure the longitudinal wave velocity of the specimen until the velocity drops suddenly. Then obtain the complete change trend of the wave velocity under different axial compression and the number (N') of the cycle impacts corresponding to the intermediate value of the specimen damage at the low-speed development stage.

(3) Preparation of pre-damaged samples. Under different axial pressures (0, 15, 25, 35 MPa), 8 groups of 50 mm high grey sandstone samples are cyclically impacted, and the bullet launching air pressure is adjusted so that the single impact incident stress wave is half sine wave with a peak value of 57.0 MPa. Stop the impact when the number of impacts reaches *N*', and these damaged specimens subjected to cyclic impact are called “pre-damaged samples”. So far, a total of 8 sets of pre-damaged samples have been obtained, and the other 4 sets of samples not subjected to cyclic impact are referred to as "intact samples" with a height of 50 mm.

(4) Uniaxial compression test and longitudinal wave velocity test during loading. 1 set of intact samples and 4 sets of pre-damaged samples are selected for uniaxial compression test, and HY-YS4A rock acoustic wave parameter tester is used at the same time to measure the axial wave velocity during the loading process. The full stress–strain curves of the intact sample, the four groups of pre-damaged samples and the corresponding relationship with the axial wave velocity are obtained.

(5) Coupled dynamic and static loading test of damaged sample and intact sample. Take 4 sets of pre-damaged samples and 4 sets of intact samples, and use the SHPB system to conduct coupled dynamic and static loading tests with different axial stresses and different incident stress waves (half sine waves with peak stresses of 95.6, 118.6, 141.3, 178.3 MPa, respectively) (axial stresses correspond to axial compression applied during the cyclic impact test) .The selected bullet is the same as that used in the cyclic impact test, and the failure mode of the sample and the dynamic stress–strain curve are obtained.

2.2 Test results of static physical and mechanical parameters

The basic physical indicators of the intact sample are obtained from the test, as listed in Table 1. The static uniaxial compression stress–strain curves of the pre-damaged sample, the intact sample and the corresponding axial longitudinal wave velocity curves are shown in Fig. 4.

The uniaxial compressive strength of the intact sample is 74.38 MPa, and the average strength of the four types of pre-damaged samples is 62.59 MPa. The stress–strain curves of several types of specimens shown in Fig. 4 can be divided into compaction stage, elastic deformation stage, crack propagation stage and failure stage. The compaction stage of the pre-damaged sample is obviously longer, mainly because the cyclic impact leads to the development of micro-cracks inside the sample. Compared with the intact sample, the pre-damaged sample has a larger plasticity and lower static compressive strength.

Table 1 Basic physical parameters of the samples

Sample number	Dry density / (g • cm^{-3})	Dry wave velocity / (m • s^{-1})	Saturated water absorption rate/ %	Sample number	Dry density / (g • cm^{-3})	Dry wave velocity / (m • s^{-1})	Saturated water absorption rate/ %
HS1-1	2.387	2 865	3.20	HS3-1	2.405	2 890	3.15
HS1-2	2.398	2 860	3.11	HS3-2	2.409	2 915	3.27
HS1-3	2.404	2 862	3.23	HS3-3	2.416	2 911	3.29
HS1-4	2.418	2 854	3.17	HS3-4	2.419	2 860	3.19
HS2-1	2.407	2 865	3.23	HS4-1	2.422	2 873	3.13
HS2-2	2.411	2 856	3.24	HS4-2	2.415	2 890	3.15
HS2-3	2.391	2 871	3.22	HS4-3	2.413	2 915	3.29
HS2-4	2.423	2 865	3.14	HS4-4	2.420	2 912	3.30

Note: The average dry density for all the samples is 2.409 g/cm^3; the average longitudinal wave velocity is 2 880 m/s; and the average saturated water absorption rate is 3.21%.

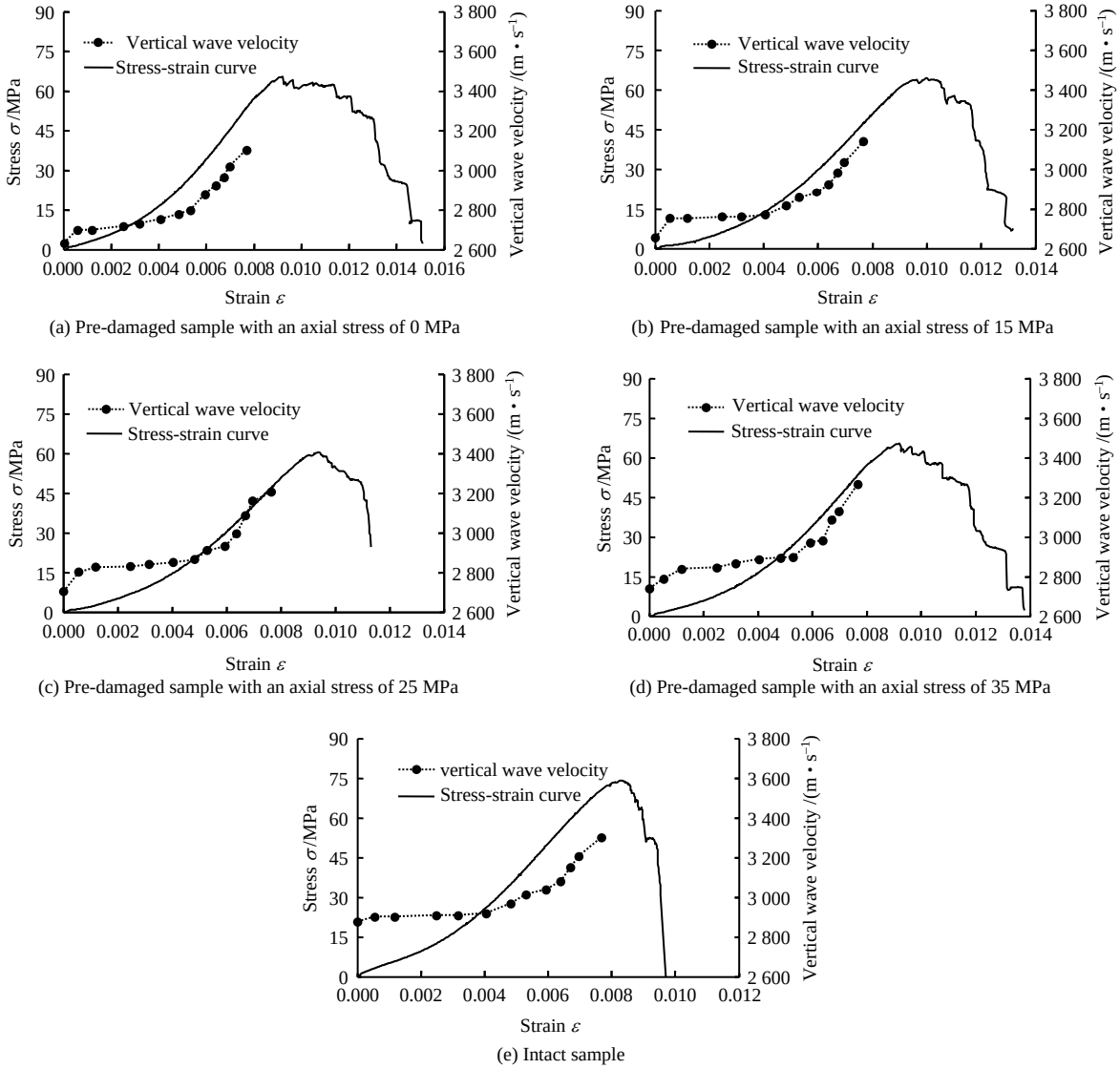

(a) Pre-damaged sample with an axial stress of 0 MPa

(b) Pre-damaged sample with an axial stress of 15 MPa

(c) Pre-damaged sample with an axial stress of 25 MPa

(d) Pre-damaged sample with an axial stress of 35 MPa

(e) Intact sample

Fig. 4 Curves of stress–strain and corresponding longitudinal wave velocities

The internal fractures of the rock and the stress state will affect the sample wave velocity[19]. Many research results indicate that the longitudinal wave velocity changes in different stages of uniaxial loading, but they all show a gradual increase in the initial stage of loading [20–21]. In this paper, the wave velocity test is carried out along the loading direction of the sample. The wave velocity testing process is limited to the compaction stage and the elastic deformation stage, and is basically limited to the crack initiation stress threshold [22]. The wave velocity measurement near the stress peak and the post-peak stage is not performed. Within the compaction stage and the linear elastic stage, the wave velocity gradually increases with the increase of stress, which is similar to the results of other researchers[23–24]. As shown in Fig.4, the sensitivity of longitudinal wave velocity of several types of samples to stress increase is roughly similar, but the initial wave velocity of pre-damaged samples is lower than that of intact samples. The greater the pre-axial compression, the higher the wave velocity corresponding to the same strain.

When the sample enters the compaction stage, the wave velocity increases slightly. This is mainly due to the initial closure of the micro-cracks inside the sample. The increase in wave velocity of several types of samples is 22–100 m/s, and the increase in intact specimens is the smallest. At this stage, the wave velocity of the pre-damaged specimen has a relatively obvious increase process, which is mainly due to the significant increase of micro-cracks inside the specimen after the pre-damage, not only parallel axial cracks, but also diagonal crack propagation (when there is axial compression, there are many such cracks). When the specimen enters the linear elastic stage and the stress increases, there is only a small increase in the longitudinal wave velocity. This is because the rock sample in this article is a typical brittle rock with a low porosity. After the pores are practically compacted, applying a low stress level cannot significantly change its internal structure. After the stress continues to increase, the longitudinal wave velocity will increase significantly. This phenomenon is mainly caused by further closure of rock cracks, especially when the holes and structures inside the rock collapse, causing the inner structure of the sample to be more encrypted[20].

3 Characteristics of sample damage evolution under cyclic impact

Macroscopic characteristic parameters such as density, elastic modulus, and longitudinal wave velocity are usually used to characterize the degree of rock damage[25]. Since the ultrasonic velocity of rock is closely related to its density and the extent of internal micro-cracks, the longitudinal wave velocity is used in this article to express the degree of damage of the specimen. During the loading process, the overall change patterns of the axial wave velocity and the transverse wave velocity of the specimen are different [23], but the wave velocity will increase in the early stage. Considering the test loading method and key factors in the analysis, this article will focus on the change in the axial wave velocity.

The damage variable D_n represented by the wave velocity is expressed as [26-27]

$$D_n = 1 - \left(\frac{V_n}{V_0} \right)^2 \quad (1)$$

where V_0 is the initial wave speed and V_n is the wave speed after damage.

The SHPB system that can apply axial stress is used for cyclic impact. The axial stress is set to be 0, 15, 25, and 35 MPa, respectively, which correspond to 0%, 20%, 33%, and 47% of the uniaxial compressive strength. After several impacts, the wave speed of the sample suddenly drops. By measuring the longitudinal wave velocity of the sample after each impact, the wave velocity V_n after different number of impacts is obtained. Using Eq.(1), the damage variable D_n after different impact times is obtained. Under different axial compressions, the relationship between the damage variable of the sample and the number of cyclic impacts is shown in Fig. 5.

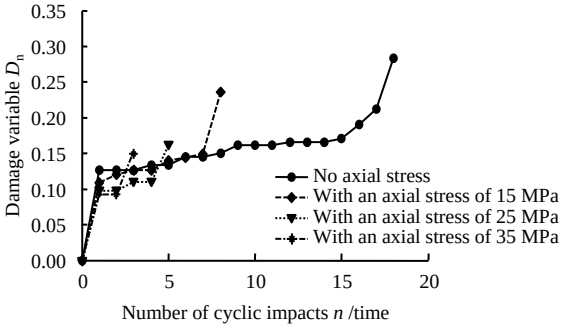

Fig. 5 Relationship between damage variable and impact number

The existence of the initial static load changes the degree of closure of the original micro-cracks inside the specimen, and different wave impedance values are formed under the same stress wave. The stress wave forms different types of action at the micro-cracks during the impact, resulting in different degrees of crack propagation of micro-cracks inside the specimen[28], which in turn causes different degrees of damage to the specimen. The inverse function of Logistic function can be used to characterize the change of rock cyclic impact damage [29]:

$$D_{01} = a_0 - \beta \ln\left(\frac{k}{n} - \eta \right) \quad (2)$$

where a_0 is the center value of the damage evolution model curve, which represents the size of the cumulative damage in the initial stage; β is the slope of the curve in the low-speed development stage of the crack; k is the value of axial static load; and η is the cumulative damage rate factor in the accelerated development stage of the crack, with a value range in（0， k/N）, and N is the total number of cyclic impacts.

According to the test results of cyclic shock wave velocity, the damage of the rock under cyclic impact with different axial stresses can be obtained by using Eq. (2), as shown in Fig. 6.

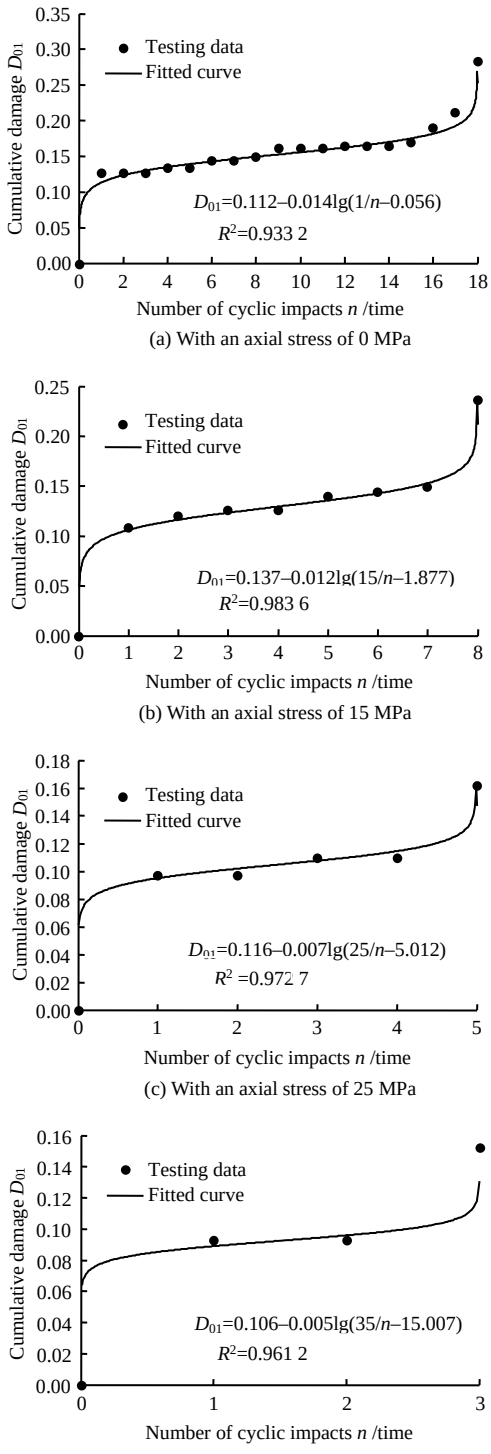

Fig. 6 Trend of damage under different axial compressions

As the number of cyclic impacts increases, the longitudinal wave velocity decreases significantly. Under different axial compression conditions, the value of the damage variable increases sharply for the first impact, and the damage changes caused by the intermediate impacts tended to be gentle. With the increase of axial pressure, the number of cyclic impacts experienced by the specimen to achieve macroscopic failure gradually decreases. When the axial pressure is 0, 15, 25, and 35 MPa, after 18, 8, 5, and 3 cycles of impact, respectively, the wave speed drops abruptly, which indicates that the specimen will be macroscopically damaged. The evolution of the damage variable value can be divided into three stages: the rapid rise stage, the stable development stage, and the sharp rise stage. Under different axial pressures, the damage variable values in the stable development stage exhibit small changes. When the axial pressure is 0 MPa, D_n changes from 0.127 to 0.171, with an average value of 0.150; when the axial pressure is 15 MPa, D_n changes from 0.109 to 0.150, with an average value. When the axial pressure is 25 MPa, D_n changes from 0.097 to 0.110, and the average value is 0.104; when the axial pressure is 35 MPa, the average value of D_n is 0.093. As the axial pressure increases, the damage caused by the first impact and the average value of D_n in the stable development stage decrease.

4 Mechanical characteristics of specimens subject to coupled dynamic and static loading

4.1 Crushing mode under coupled dynamic and static loading

Take the rock (pre-damage specimen) in the stage of stable damage development stage as the research object, set the corresponding axial pressure, and perform a strike test, i.e., a coupled dynamic and static loading test of the pre-damaged specimen is carried out. The typical incident wave (i), transmitted wave (t), and reflected wave (r) directly collected by the coupled dynamic and static loading test are shown in Fig. 7, and the superposition of the incident wave and the reflected wave is in good agreement with the transmitted wave, indicating that the test in this paper satisfies stress uniformity assumption. The failure modes of pre-damaged specimens and intact specimens under different incident waves (half sine waves with peak stresses of 95.6, 118.6, 141.3 and 178.3 MPa, respectively) and axial compressions of 0 and 35 MPa are shown in Fig. 8.

As the peak value of the incident wave increases, the sample is more broken, and the tensile failure mode appears when the axial pressure is 0 MPa. The frictional resistance between the rod and the specimen under the influence of axial pressure cannot be ignored. The specimen under the effect of axial pressure is generally in compression (tension) shear failure mode. When the incident wave and axial pressure are the same, the pre-damaged sample is broken more than the intact sample. The incident wave is the same, and the degree of breakage of the intact and pre-damaged specimens varies with different axial pressures. The pre-damaged specimens are relatively more broken at 0 MPa axial pressure.

4.2 Analysis of the strength in coupled dynamic and static loading

The dynamic stress–strain curves of the pre-damaged specimen and the intact specimen under different axial pressures and different peak incident waves are obtained through coupled dynamic and static tests. Take the test results of 0 and 35 MPa axial compression as an example for analysis, as shown in Fig. 9.

The stress–strain curves of the two types of specimens under combined dynamic and static loading have no obvious compaction stage, mainly because the internal micro-cracks of the specimen are too late to close and the rock crystals show greater inertia under the impact load. There is no obvious correlation between the slope of the linear elastic stage (elastic modulus) and impact velocity[30]. Axial pressure has a great influence on peak and post-peak morphology. Post-peak (failure stage) curves are divided into three types, namely "post-peak plasticity", "stress drop", and "strain rebound". When the axial pressure is within a certain stress level[31], the internal micro-cracks of the rock sample are closed, the damage variable is reduced, and the elastic modulus increases compared with the case of no axial compression. Under the same loading condition, the strength of the pre-damaged specimen is smaller and the plasticity is larger.

Figure 10 shows the relationships between the dynamic compressive strength and strain rate of the pre-damaged and intact specimens under different axial compressions.

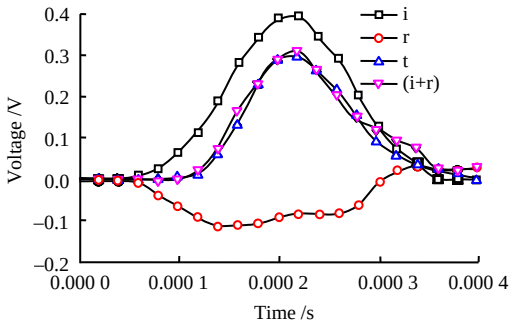

Fig. 7 Curves of typical incident wave (i), reflected wave (r) and transmitted waves (t)

The peak stress is 95.6 MPa The peak stress is 118.6 MPa The peak stress is 141.3 MPa The peak stress is 178.3 MPa

(a) Pre-damaged specimen with an axial pressure of 0 MPa

The peak stress is 95.6 MPa The peak stress is 118.6 MPa The peak stress is 141.3 MPa The peak stress is 178.3 MPa

(b) Intact specimen with an axial pressure of 0 MPa

The peak stress is 95.6 MPa The peak stress is 118.6 MPa The peak stress is 141.3 MPa The peak stress is 178.3 MPa

(c) Pre-damaged specimen with an axial pressure of 35 MPa

The peak stress is 95.6 MPa The peak stress is 118.6 MPa The peak stress is 141.3 MPa The peak stress is 178.3 MPa

(d) Intact specimen with an axial pressure of 35 MPa

Fig. 8 Photos of damaged samples under different incident waves

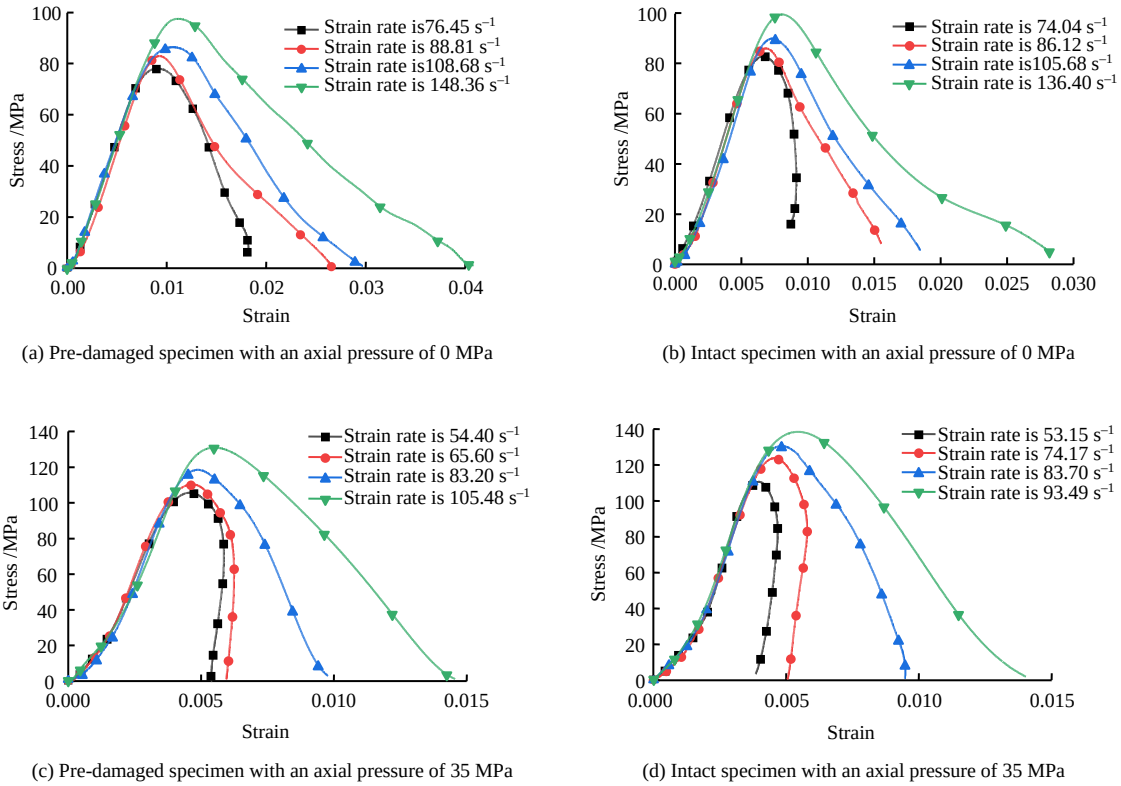

(a) Pre-damaged specimen with an axial pressure of 0 MPa

(b) Intact specimen with an axial pressure of 0 MPa

(c) Pre-damaged specimen with an axial pressure of 35 MPa

(d) Intact specimen with an axial pressure of 35 MPa

Fig. 9 Curves of typical stress–strain

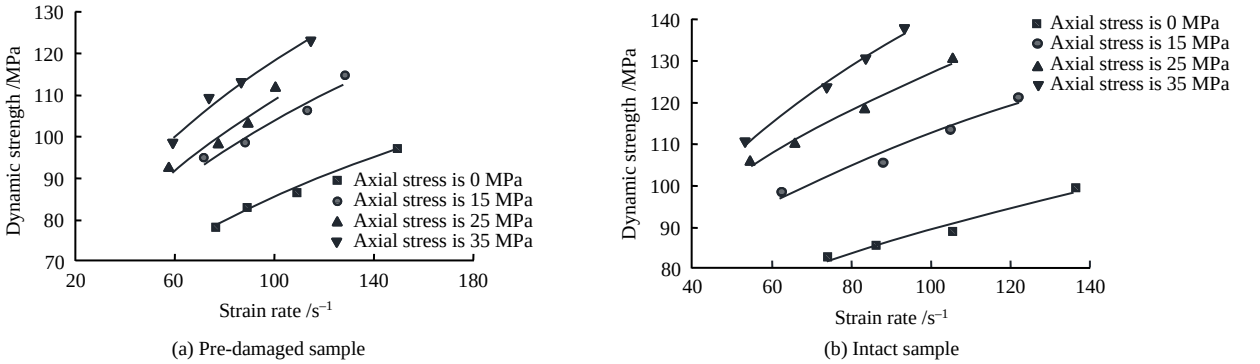

(a) Pre-damaged sample (b) Intact sample

Fig. 10 Relationship between dynamic compressive strength and strain rate

Both the pre-damaged and intact specimens show obvious strain rate effects, and the dynamic compressive strength increases with the increase of strain rate. The relationship between dynamic compressive strength and strain rate can be expressed by an exponential function as

$$\sigma_{\mathrm{d}} = a\dot{\varepsilon}^{b} \tag{3}$$

where σ_{d} is the dynamic compressive strength of the rock (MPa); and $\dot{\varepsilon}$ is the strain rate (1/s). Under different conditions, values of parameters *a* and *b* are shown in Table 2.

Table 2 Values of parameters *a* and *b*

Type of samples	Axial stress / MPa	Value of parameter *a*	Value of parameter *b*
Pre-damaged samples	0	19.50	0.290
	15	23.36	0.320
	25	25.14	0.325
	35	22.05	0.341
Intact samples	0	22.64	0.299
	15	26.54	0.318
	25	28.87	0.326
	35	23.75	0.386

The value of parameter *b* is about 0.3, which is consistent with conclusions of other researchers[32]. The strain rate enhancement effect of intact rock is more significant. In this experiment, under the same strain rate, the dynamic compressive strength of the pre-damaged and intact specimens increases with the increase of axial compression, and the axial compression of 35 MPa does not exceed 50% of the static strength. Therefore, the strength does not decrease with the increase of axial compression, and maybe the dynamic compressive strength will decrease only when the axial compression exceeds about 70% of the static strength [31, 33–34].

Rock is a polymer in which various mineral particles are bonded or cemented together. When it is subjected to an impact dynamic load, the connection (bonding) force between the mineral particles is weakened, causing the cohesion and internal friction angle of the rock sample to decrease, which further leads to deterioration of mechanical properties. With the increase of the number of cyclic impacts, the randomly generated damage field or weak surface within the rock sample gradually increases, and this change is irrecoverable even if it is within the elastic limit range [2]. Cyclic impact causes the development of micro-cracks in the rock. The impact damage of the rock is caused by the expansion of cracks. The energy required for crack generation is much higher than the energy required for crack propagation. The dynamic characteristics of the pre-damaged specimen are different from that of the intact specimen, which is a reflection of the generation and propagation of micro-cracks inside the specimen, and the dynamic strength and energy absorption capacity of the pre-damaged specimen are significantly reduced. The dynamic strength of rock increases with the increase of strain rate, but due to the influence of the pre-damaged effect of cyclic impact, the effect of strain rate enhancement is slightly weakened.

5 Dynamic constitutive model of pre-damaged specimen under one-dimensional static load

5.1 Establishment and verification of the constitutive model

According to the strain equivalence principle proposed by Lemaitre[35] and the strain equivalence principle promoted by Zhang et al. [36], the total rock damage variable after cyclic impact and combined dynamic and static loading is obtained as

$$D_1 = D + D_0 - DD_0 \tag{4}$$

where D_1 is the total damage variable of the rock under the cyclic impact and coupled dynamic and static loading; *D* is the damage variable caused by the impact dynamic load; D_0 is the initial damage of the rock before impacted, including the cyclic impact damage D_{01} and the pre-load static damage D_{02} of the coupled dynamic and static loading test, which means, $D_0 = D_{01} + D_{02}$.

The strength of the rock obeys the Weibull statistical distribution, and the load damage factor of the rock is expressed as[37]

$$D = 1 - \exp\left[-\left(\frac{\varepsilon}{\alpha}\right)^{m}\right] \tag{5}$$

where *m* is the shape parameter; and α is the material parameter.

Substituting Eq. (5) into Eq. (4) leads to the total damage evolution equation as

$$D_1 = 1-(1-D_0)\exp\left[-\left(\frac{\varepsilon}{\alpha}\right)^m\right] \tag{6}$$

In other words,

$$D_1 = 1-(1-D_{01}-D_{02})\exp\left[-\left(\frac{\varepsilon}{\alpha}\right)^m\right] \tag{7}$$

The constitutive equation of the rock can be expressed as

$$\sigma = E_0(1-D_1)\varepsilon \tag{8}$$

where E_0 is the dynamic modulus of elasticity.

Substituting Eq. (7) into Eq. (8), we get

$$\sigma = E_0\varepsilon(1-D_{01}-D_{02})\exp\left[-\left(\frac{\varepsilon}{\alpha}\right)^m\right] \tag{9}$$

Substituting Eq. (2) into Eq. (9), we get

$$\sigma = E_0\varepsilon\left[1-D_{02}-a_0+\beta\ln\left(\frac{k}{n}-\eta\right)\right]\exp\left[-\left(\frac{\varepsilon}{\alpha}\right)^m\right] \tag{10}$$

Equation (10) is the dynamic constitutive equation of the pre-damaged specimen under axial compression.

With reference to the idea of literature[37], combined with the characteristics of the dynamic stress–strain curve, Eq. (10) satisfies the following four conditions:

① when $\varepsilon = 0$, $\sigma = 0$

② when $\varepsilon = 0$, $\dfrac{\mathrm{d}\sigma}{\mathrm{d}\varepsilon} = E$

③ when $\varepsilon = \varepsilon_{\max}$, $\sigma = \sigma_{\max}$

④ when $\varepsilon = \varepsilon_{\max}$, $\dfrac{\mathrm{d}\sigma}{\mathrm{d}\varepsilon} = 0$

Since the impact stress–strain curve basically has no compaction stage, condition ② meets the characteristics of the dynamic stress–strain curve.

Both sides of Eq.(9) being differentiated by strain results in

$$\mathrm{d}\sigma/\mathrm{d}\varepsilon = E_0(1-D_{01}-D_{02})\exp\left[-\left(\frac{\varepsilon}{\alpha}\right)^m\right]\left[1-\left(\frac{\varepsilon}{\alpha}\right)^m\right] \tag{11}$$

From condition ②, we can get

$$E = E_0(1-D_{01}-D_{02}) \tag{12}$$

Therefore, it can be seen that in Eqs. (9) and (10), E_0 is the dynamic elastic modulus of the intact sample.

From condition ③ and Eq. (9), we can get

$$\frac{\sigma_{\max}}{E_0(1-D_{01}-D_{02})\varepsilon_{\max}} = \exp\left[-\left(\frac{\varepsilon_{\max}}{\alpha}\right)^m\right] \tag{13}$$

Taking logarithms twice on both sides of Eq.(13) results in

$$\ln\left[\ln\frac{E_0(1-D_{01}-D_{02})\varepsilon_{\max}}{\sigma_{\max}}\right] = m\ln\left(\frac{\varepsilon_{\max}}{\alpha}\right) \tag{14}$$

According to condition ④ and Eq. (11), we get

$$\left[1-\left(\frac{\varepsilon}{\alpha}\right)^m\right] = 0 \tag{15}$$

That is

$$\frac{1}{m} = \left(\frac{\varepsilon_{\max}}{\alpha}\right)^m \tag{16}$$

Taking the logarithm on both sides of Eq.(16) yields

$$\ln\left(\frac{1}{m}\right) = m\ln\left(\frac{\varepsilon_{\max}}{\alpha}\right) \tag{17}$$

Comparing Eqs. (14) and (17), we find that the right sides of the two equations are equal, that is

$$m = \frac{1}{\ln\left(\dfrac{E_0(1-D_{01}-D_{02})\varepsilon_{\max}}{\sigma_{\max}}\right)} \tag{18}$$

Substituting Eq. (18) into Eq. (16), we get

$$a = \frac{\varepsilon_{\max}}{(1/m)^{\frac{1}{m}}} \tag{19}$$

The Eq. (10) contains 7 parameters such as $n, a_0, \beta, k, \eta, \alpha$, and m, which can be all obtained through the above analysis. The initial damage parameter $D_0 = D_{01} + D_{02}$ is included in the constitutive relationship expression, and D_0 can be a negative value. Among them, D_{01} is the cyclic impact damage parameter, which is generally a positive value, and D_{02} is the axial compression damage parameter, which can be a positive value or a negative value. Based on the results of many coupled dynamic and static tests of rocks [8, 31], it can be found that if the axial pressure does not exceed a certain threshold, D_{02} is taken as a negative value (the pre-added axial pressure in the test in this article did not exceed the threshold). If it exceeds the threshold, D_{02} is taken as a positive value, which is also one of the main reasons why the dynamic compressive strength first increases and then decreases with the increase of axial pressure. Obviously, only the changes of the values of D_{01} and D_{02} directly affect the pre-peak and post-peak slope of the stress–strain curve, but the changes of the values of D_{01} and D_{02} will also cause the changes of the values of $\sigma_{\max}$ and $\varepsilon_{\max}$ at the same time. Therefore, the influence of the values of D_{01} and D_{02} on the stress–strain relationship is more complicated.

The constitutive model is verified with typical test data of intact or pre-damaged specimens under different axial pressures, different peak incident waves. The fitting curve is consistent with the measured curve, as shown in Fig. 11. Based on the consideration of the test process

and related control factors, the constitutive relationship established in this paper is only applicable to the situation when the pre-axial compression is within the elastic deformation stage (or within the crack initiation stress threshold of the uniaxial test).

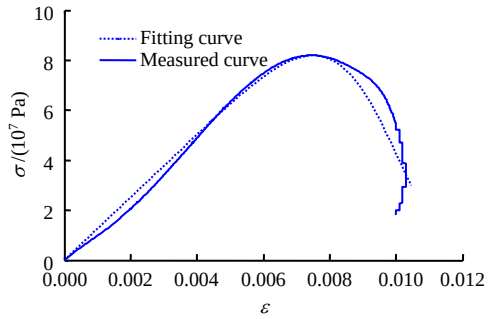

(a) 0 MPa axial compression–intact sample–peak 95.6 MPa–incident wave

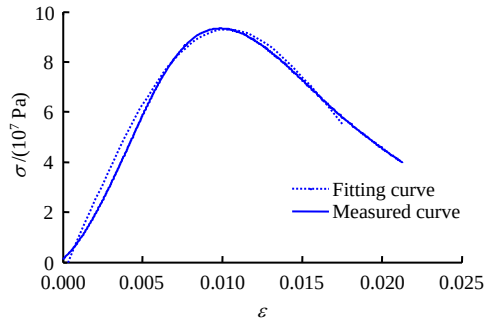

(b) 15 MPa axial compression–pre-damaged sample–peak 118.6 MPa– incident wave

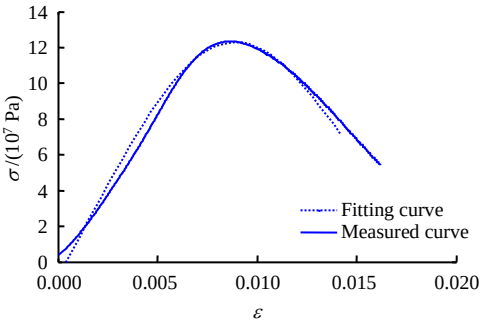

(c) 35 MPa axial compression–pre-damaged sample–peak 141.3 MPa– incident wave

Fig. 11 Comparison between stress–strain measured and fitting curves

5.2 Mechanical characteristics analysis of coupled dynamic and static loading damage

In the SHPB test, the rock wave velocity after pre-loading can be obtained from Fig. 4. According to Eq. (1), the value of the pre-loading damage variable is shown in Table 3.

Values of rock damage variables D_{01} and D_{02} under the dynamic and static coupling load are provided in Table 4. According to Table 4 and the values of σ_{max} and ε_{max} in the stress–strain curve, the development trend of damage variables under coupled dynamic and static loading conditions (see Fig. 12) and the comparison of damage variables between typical intact specimens and pre-damaged specimens (see Fig. 13) can be obtained.

Table 3 Values of wave velocity and D_{02}

Types of samples	Axial stress / MPa	Initial wave speed of uniaxial test/ (m · s^{-1})	Wave speed corresponding to pre-added axial force/ (m · s^{-1})	value of D_{02}
Pre-damaged samples	0	2 635	2 635	0.000
	15	2 654	2 725	–0.054
	35	2 703	3 011	–0.241
	45	2 742	3 304	–0.452
Intact samples	0	2 880	2 880	0.000
	15	2 880	3 023	–0.102
	35	2 880	3 213	–0.245
	45	2 880	3 315	–0.325

Table 4 Values of D_{01} and D_{02}

Axial stress / MPa	Pre-damaged samples			Intact samples		
	D_{01}	D_{02}	D_0	D_{01}	D_{02}	D_0
0	0.150	0.000	0.150	0.000	0.000	0.000
15	0.130	–0.054	0.076	0.000	–0.102	–0.102
25	0.110	–0.172	–0.062	0.000	–0.175	–0.175
35	0.100	–0.352	–0.251	0.000	–0.253	–0.253

The damage evolution curve can reflect the meso-mechanical response of the rock, and is consistent with the macroscopic failure and deformation process of the specimen. In general, the damage variable gradually increases with the increase of strain. The damage evolution curves are all in the shape of "S" and are divided into three stages. ①When the strain is 0, the initial damage variable of the intact specimen is 0, and the damage variable shows almost no increase in the initial stage. This is because the loading stress is much smaller than the elastic limit of the specimen when it is in the initial elastic stage. At this time, there is almost no damage to the specimen and only elastic strain occurs. ②The concave section of the damage evolution curve corresponds to the plastic deformation stage, the damage variable rises rapidly, the crack propagation speed increases, and the specimen begins to exhibit plastic yield. With the increase of strain, the micro-cracks inside the specimen continue to expand, and the damage variable continues to increase. When the crack growth reaches the critical failure state, i.e., corresponding to the peak stress of the dynamic stress–strain curve, the damage variable increases fastest, and unstable crack propagation occurs. The strain corresponding to the concave-convex inflection point of the damage variable curve is consistent with the peak strain of the dynamic stress-strain curve. ③The convex section of the damage evolution curve corresponds to the strain softening stage, and the slope of the curve gradually decreases. At this time, the internal cracks of the specimen increase, and finally the specimen macroscopically fractures. At this time, the damage variable tends to 1. With the increase of the peak value of the incident wave, the maximum slope of the damage curve, that is, the slope of the curve at the convex concave inflection point, increases. The damage corresponding to the peak strain of the dynamic stress-strain curve increases with the

increase of the peak value of the incident wave. The macroscopic appearance is that the rock is more broken.

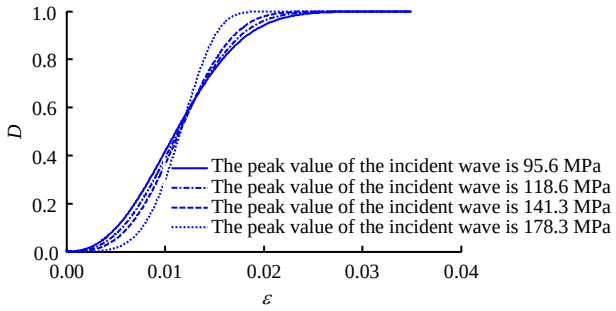

(a) 0 MPa axial stress–intact specimen

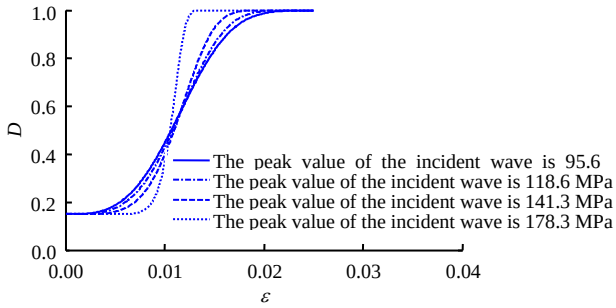

(b) 0 MPa axial stress–pre-damaged specimen

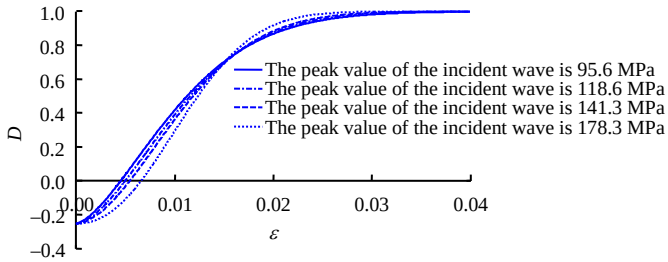

(c) 35 MPa axial compression–intact specimen

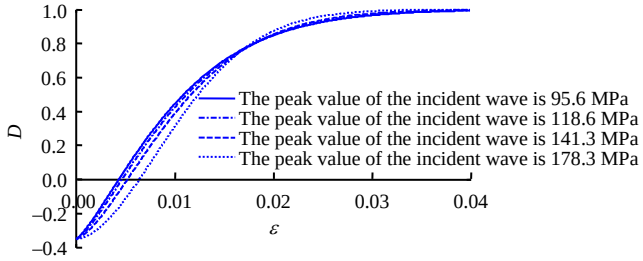

(d) 35 MPa axial compression–pre-damaged specimen

Fig. 12 Curves of damage value under different incident plane waves

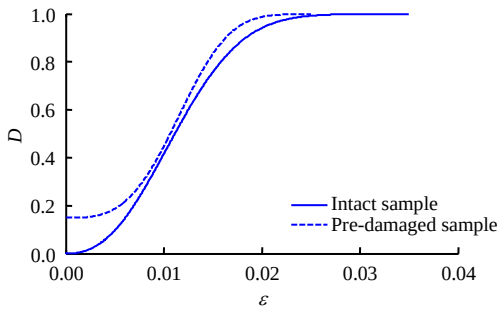

Fig. 13 Damage values comparison between the pre-damaged and intact samples in the conditions of a 0 MPa axial compression, 95.6 MPa and incident wave

The damage evolution process of the pre-damaged specimen is obviously different from that of the intact rock. The initial damage variable of the pre-damaged specimen is not 0, which indicates that a certain degree of damage and degradation has been experienced before dynamic loading. Compared with the intact rock, the value of the damage variable of the pre-damaged specimen at the same strain is slightly larger, which can reflect the higher degree of internal deterioration of the pre-damaged rock, and macroscopically, the stiffness and strength of the pre-damaged specimen are reduced. At the same time, when the damage degree is the same, the strain of the pre-damaged rock is smaller, that is, the damage accumulation rate of the pre-damaged rock is faster, and the plasticity of the rock is weaker.

During the coupled dynamic and static loading process, after pre-axial compression, the initial value of the rock damage variable may appear negative. At this time, the initial horizontal section of the damage variable curve is very short and it quickly enters the rapid growth stage of damage, indicating that when the sample is in the coupled dynamic and static loading process, the initial linear elastic stage is shorter, and the microcracks inside the sample begin to expand under a smaller dynamic stress level, and then the damage degree of the sample gradually increases to the inflection point of the curve. The maximum slope of the damage variable curve of the pre-damaged specimen under the same incident wave and the same static load condition is larger, and the degree of specimen fracture will be higher. Under 35 MPa axial compression, when the damage variable of the pre-damaged specimen is 0.34, it corresponds to the peak stress, and then the strain increases more than that in the case without axial compression, indicating that the specimen has greater plasticity. When the axial pressure is within a certain value, as the axial pressure increases, the dynamic strength increases. The axial pressure inhibits the expansion of the cracks perpendicular to the axial direction and makes the original cracks inside the sample closed. The micro cracks are closed, and the pores are further compacted and collapsed. These affect the wave impedance, thereby changing the dynamic strength of the rock under axial compression.

6 Conclusion

(1) During the uniaxial loading process, the change of longitudinal wave velocity is closely related to the stress. Within the compaction stage and the linear elastic stage, the wave velocity gradually increases with the increase of stress, and the pre-damaged specimen wave velocity increases significantly during the compaction process. The initial wave velocity of the pre-damaged specimen is lower than that of the intact specimen. The larger the pre-axial compression, the higher the wave velocity corresponding to the same strain.

(2) In the process of cyclic impact, the degree of damage in the specimens with different initial static loads is different. As the axial pressure increases, the damage caused by the first impact and the average

value of the damage variables in the stable development stage are reduced. The inverse function of Logistic function can be used to characterize the change of rock cyclic impact damage, which is generally divided into three stages: the rapid rise stage, the stable development stage, and the sharp rise stage.

(3) Both the pre-damaged and intact specimens show a strong strain rate effect. The dynamic compressive strength increases with the increase of the strain rate. The relationship between the dynamic compressive strength and the strain rate can be expressed in the form of an exponential function $\sigma_{\mathrm{d}} = a\dot{\varepsilon}^{b}$, and the value of the parameter *b* is around 0.3, the strain rate enhancement effect of the intact rock is more significant.

(4) In the coupled dynamic and static loading, when the incident wave and axial pressure are the same, the pre-damaged sample is more broken than the intact sample. When the incident wave is the same, the degree of breakage of the intact and pre-damaged specimens is different with different axial pressures. The pre-damaged specimens are relatively broken at 0 MPa axial pressure, and the existence of axial pressure can cause an increase in the elastic modulus. Under the same load condition, the strength of the pre-damaged specimen is smaller, and the plasticity is larger.

(5) The established constitutive relationship including the pre-damage and static load damage variables shows good consistency with the measured curve. The obtained total damage variable curve can not only explain the consistency of the macroscopic and meso-damage processes of the rock, but also reflect the non-linear effects of two factors, namely, cyclic impact and static preload, on the development of total rock damage. The constitutive relationship presented in this paper is only applicable to the situation when the preload axial stress is within the crack initiation stress threshold of the uniaxial test. In the constitutive relationship, the influence of the value of D_{01} and D_{02}, on the stress–strain relationship is more complicated, and the initial damage parameter D_0 can be negative, which is also one of the main reasons for the increase of dynamic strength with the increase of axial compression.

References

[1] LI H B, XIA X, LI J C, et al. Rock damage control in bedrock blasting excavation for a nuclear power plant[J]. International Journal of Rock Mechanics and Mining Sciences, 2011, 48(2): 210–218.

[2] DENG Hong-wei, LIU Chuan-ju, KE Bo, et al. Experimental study on microscopic damage characteristics of granite under cyclic dynamic disturbances[J]. Chinese Journal of Engineering, 2017, 39(11): 1634–1639.

[3] FAN Xiu-feng, JIAN Wen-bin. Experimental research on fatigue characteristics of sandstone using ultrasonic wave velocity method[J]. Chinese Journal of Rock Mechanics and Engineering, 2008, 27(3): 557–563.

[4] LU Hua. Research on dynamic responses and damage effect of red sandstone with fluid-solid coupling under impact loading[D]. Beijing: China University of Mining and Technology, 2013.

[5] MEI Nian-feng. Research on fatigue damage and mechanical characteristics of brittle rock under cycle dynamic loading[D]. Wuhan: China University of Geosciences, 2014.

[6] LÜ Xiao-cong, XU Jin-yu, GE Hong-hai, et al. Effects of confining pressure on mechanical behaviors of sandstone under dynamic impact loads[J]. Chinese Journal of Rock Mechanics and Engineering, 2010, 29(1): 193–201.

[7] XIAO J Q, DING D X, XU G, et al. Inverted S-shaped model for nonlinear fatigue damage of rock[J]. International Journal of Rock Mechanics and Mining Sciences, 2009, 46(3): 643–648.

[8] GONG Feng-qiang. Experimental study of rock mechanical properties under coupled static-dynamic loads and dynamic strength criterion[D]. Changsha: Central South University, 2010.

[9] CHRISTENSON R J, SWANSON S R, BROWN W S. Split-Hopkinson-bar tests on rock under confining pressure[J]. Experimental Mechanics, 1972, 12 (11): 508–513.

[10] ZHOU Zi-long. Study on experimental and mechanical behaviors of rock under static-dynamic coupling loads[D]. Changsha: Central South University, 2007.

[11] LI X B, ZHOU Z L, LOK T S, et al. Innovative testing technique of rock subjected to coupled static and dynamic loads[J]. International Journal of Rock Mechanics and Mining Sciences, 2008, 45(5): 739–748.

[12] LI Xi-bing, ZUO Yu-jun, MA Chun-de. Constitutive model of rock under coupled static-dynamic loading with intermediate strain rate[J]. Chinese Journal of Rock Mechanics and Engineering, 2006, 25(5): 865–874.

[13] LIU Shao-hong, QIN Zi-han, LOU Jin-fu. Experimental study of dynamic failure characteristics of coal-rock compound under one-dimensional static and dynamic loads[J]. Chinese Journal of Rock Mechanics and Engineering, 2014, 33(10): 2064–2075.

[14] WEN Lei, LI Xi-bing, WU Qiu-hong, et al. Dynamic strength of granite porphyry under freezing-thawing cycles[J]. Chinese Journal of Rock Mechanics and Engineering, 2015, 34(7): 1297–1306.

[15] YIN Tu-bing. Study on dynamic behavior of rocks considering thermal effect[D]. Changsha: Central South University, 2012.

[16] YANG Fu-jian, HU Da-wei, ZHOU hui, et al. Study on physical and mechanical properties of granite after dynamic disturbance[J]. Chinese Journal of Rock Mechanics and Engineering, 2018, 37(6): 1459–1467.

[17] Yangtze River Scientific Research Institute, Changjiang

Water Resources Commission. SL264—2001 Specifications for rock tests in water conservancy and hydroelectric engineering[S]. Beijing: China Water Power Press, 2001.

[18] HUANG Li-xing. Development and new achievements of rock dynamics in China[J]. Rock and Soil Mechanics, 2011, 32(10): 2889–2900.

[19] ULLEMEYER K, SIEGESMUND S, RASOLOFOSAON P N J, et al. Experimental and texture-derived P-wave anisotropy of principal rocks from the transalp traverse: an aid for the interpretation of seismic field data[J]. Tectonophysics, 2006, 414: 97–116.

[20] LIU Zu-yuan, HU Yu-liang, CHEN Yong. Ultrasonic P-wave attenuation in dry and saturated rocks under uniaxial compression[J]. Acta Geophysica Sinica, 1984, 27(4): 349–359.

[21] ZHENG Gui-ping, ZHAO Xing-dong, LIU Jian-po, et al. Experimental study on change in acoustic wave velocity when rock is loading[J]. Journal of Northeastern University (Natural Science), 2009, 30(8): 1197–1200.

[22] ZHANG Guo-kai, LI Hai-bo, XIA Xiang, et al. Experiment study on acoustic emission and wave propagation in granite under uniaxial compression[J]. Chinese Journal of Rock Mechanics and Engineering, 2017, 36(5): 1133–1144.

[23] HU Ming-ming, ZHOU Hui, ZHANG Yong-hui, et al. Analysis of acoustic property of sandstone under uniaxial loading[J]. Rock and Soil Mechanics, 2018, 39(12): 4468–4474.

[24] LI Hao-ran, YANG Chun-he, LIU Yu-gang. Experimental research on ultrasonic velocity and acoustic emission properties of granite under failure process[J]. Chinese Journal of Geotechnical Engineering, 2014, 36(10): 1915–1923.

[25] ZHAO Ming-jie, WU De-lun. Ultrasonic velocity and attenuation of rock under uniaxial loading[J]. Chinese Journal of Rock Mechanics and Engineering, 1999, 18(1): 50–54.

[26] JIN Jie-fang, LI Xi-bing, WANG Guan-shi, et al. Failure modes and mechanisms of sandstone under cyclic impact loadings[J]. Journal of Central South University (Science and Technology), 2012, 43(4): 1453–1461.

[27] XIE He-ping. Rock concrete damage mechanics[M]. Xuzhou: China University of Mining and Technology Press, 1990: 152–166.

[28] LI Qing, ZHANG Xi, LI Sheng-yuan, et al. Experimental study of dynamic fracture behaviors of branched cracks under blasting stress wave[J]. Rock and Soil Mechanics, 2011, 32(10): 3026–3032.

[29] JIN Jie-fang, LI Xi-bing, QIU Can, et al. Evolution model for damage accumulation of rock under cyclic impact loadings and effect of static loads on damage evolution[J]. Chinese Journal of Rock Mechanics and Engineering, 2014, 33(8): 1662–1671.

[30] SHAN Ren-liang, XUE You-song, ZHANG Qian. Time dependent damage model of rock under dynamic loading[J]. Chinese Journal of Rock Mechanics and Engineering, 2003, 22(11): 1771–1776.

[31] LI Xi-bing, GONG Feng-qiang, GAO Ke, et al. Test study of impact failure of rock subjected to one-dimensional coupled static and dynamic loads[J]. Chinese Journal of Rock Mechanics and Engineering, 2010, 29(2): 251–260.

[32] LI X B, LOK T S, ZHAO J. Dynamic characteristics of granite subjected to intermediate loading rate[J]. Rock Mechanics and Rock Engineering, 2005, 38(1): 21–39.

[33] GONG F Q, SI X F, LI X B, et al. Dynamic triaxial compression tests on sandstone at high strain rates and low confining pressures with split Hopkinson pressure bar[J]. International Journal of Rock Mechanics and Mining Sciences, 2019, 113(1): 211–219.

[34] GONG Feng-qiang, LI Xi-bing, LIU Xi-ling, et al. Experimental study of dynamic characteristics of sandstone under one-dimensional coupled static and dynamic loads[J]. Chinese Journal of Rock Mechanics and Engineering, 2010, 29(10): 2076–2085.

[35] LEMATIRE J. How to use damage mechanics[J]. Nuclear Engineering & Design, 1984, 80(1): 233–245.

[36] ZHANG Quan-sheng, YANG Geng-she, REN Jian-xi. New study of damage variable and constitutive equation of rock[J]. Chinese Journal of Rock Mechanics and Engineering, 2003, 22(1): 30–34.

[37] WU Zheng, ZHANG Chen-juan. Investigation of rock damage model and its mechanical behaviour[J]. Chinese Journal of Rock Mechanics and Engineering, 1996, 15(1): 55–61.